Synthesis and Cyclic Voltammetry of Trinuclear Sulphido Clusters of Nickel(II), Palladium(II) and Platinum(II) and Selenido Clusters of Nickel(II) with 1,2-Bis(diphenylphosphino)ethane, and Crystal Structures of Sulphido and Selenido Clusters of Nickel(II)†

Keiji Matsumoto,* Norihiko Saiga, Shigeki Tanaka and Shun'ichiro Ooi
Department of Chemistry, Faculty of Science, Osaka City University, Sumiyoshi-ku, Osaka 558, Japan

The reaction between M^{2+}(M = Ni, Pd or Pt), 1,2-bis(diphenylphosphino)ethane (dppe), and NaSH or NaSeH in acetonitrile affords the trinuclear clusters $[Ni_3S_2(dppe)_3][BPh_4]_2$·MeCN **1** $[Ni_3Se_2(dppe)_3][BPh_4]_2$ **2**, $[Pd_3S_2(dppe)_3][PF_6]_2$ **3**, and $[Pt_3S_2(dppe)_3][PF_6]_2$·MeCN **4**. The X-ray structures of $[Ni_3S_2(dppe)_3][PF_6]_2$·MeCN and **2** were determined and cyclic voltammograms of **1**–**4** recorded. The structures of $[Ni_3S_2(dppe)_3]^{2+}$ and $[Ni_3Se_2(dppe)_3]^{2+}$ comprise three square-planar NiE_2P_2(E = S or Se) co-ordination planes sharing two μ_3-E ligands. The Ni–E, Ni···Ni, and E···E lengths for $[Ni_3S_2(dppe)_3]^{2+}$ are 2.192, 2.827 and 2.924(6) Å, while for **2** they are 2.311, 3.004 and 3.051(4) Å, indicating a smaller central Ni_3S_2 core for $[Ni_3S_2(dppe)_3]^{2+}$ than the Ni_3Se_2 core of **2**. Cyclic voltammograms of complexes **1** and **2** in dimethylformamide (dmf) at 293 K give two reduction peaks with associated oxidation peaks. Moreover, a broad oxidation peak appears at −0.87 V for **1**. Two couples at −1.64 and −2.04 for **1** and at −1.59 and −1.87 V for **2** are reversible in acetonitrile solution at 255 K. The cyclic voltammogram of **3** in dmf gives only one reduction peak at a scan rate of 50 mV s^{-1} at 293 K, but at 255 K a reversible couple is exhibited at −1.96 V. A reduction peak at −2.10 V with an associated smaller oxidation peak at −2.07 V is observed for **4** in dmf at a scan rate of 50 mV s^{-1} at 293 K.

The reaction of $NiCl_2$ with sulphide ion usually gives an unsoluble binary sulphide. In the presence of thiolate, however, several trinuclear nickel sulphide thiolate clusters[1–4] have been isolated and structurally characterized. On the other hand, the synthesis, structures,[5–8] and reaction[9] of trinuclear nickel clusters with sulphide and phosphine ligands have also been reported. Electrochemical studies on these clusters have, however, not been made.

As an investigation of the reaction systems MCl_2(M = Ni or Pt) or $Pd(MeCO_2)_2$–1,2-bis(diphenylphosphino)ethane (dppe)–NaSH or NaSeH gave trinuclear clusters $[Ni_3S_2(dppe)_3][BPh_4]_2$·MeCN **1**, $[Ni_3Se_2(dppe)_3][BPh_4]_2$ **2**, $[Pd_3S_2(dppe)_3][PF_6]_2$ **3**, and $[Pt_3S_2(dppe)_3][PF_6]_2$·MeCN **4**, we describe here the synthesis, X-ray structures, and cyclic voltammograms of the complexes.

Experimental

All operations were carried out in a dry nitrogen atmosphere using solvents degassed prior to use. Acetonitrile and dichloromethane were dried over CaH_2 and molecular sieve type 4A respectively and distilled. The salts NaSH[10] and NaSeH[11] were prepared by the literature methods.

Preparations.—$[Ni_3S_2(dppe)_3][BPh_4]_2$·MeCN **1**. To a stirred suspension of $NiCl_2$(1 mmol, 130 mg) in MeCN (20 cm^3) was added dppe (1 mmol, 410 mg). After 3 h, NaSH (0.8 mmol, 45 mg) was added and the solution was stirred for 20 h. The resulting dark brown solution was treated with $NaBPh_4$ (0.6 mmol, 200 mg) and filtered. Dark brown crystals of $[Ni_3S_2(dppe)_3][BPh_4]_2$·MeCN were obtained in 22% yield (155 mg) upon standing the filtrate at room temperature for 2 d in the air (Found: C, 72.5; H, 5.5; N, 0.6, $C_{128}H_{115}B_2NNi_3P_6S_2$ requires C, 72.7; H, 5.5; N, 0.7%). The complex $[Ni_3S_2(dppe)_3][PF_6]_2$·MeCN was prepared by an analogous method using $NaPF_6$ (1 mmol, 160 mg) instead of $NaBPh_4$. Yield 110 mg (19%) (Found: C, 54.3; H, 4.3; N, 0.7. $C_{80}H_{75}F_{12}NNi_3P_8S_2$ requires C, 54.4; H, 4.3, N, 0.8%).

$[Ni_3Se_2(dppe)_3][BPh_4]_2$ **2**. To a suspension of $NiCl_2$ (1 mmol, 130 mg) in MeCN (10 cm^3) and CH_2Cl_2 (10 cm^3) was added dppe (1 mmol, 400 mg). After stirring for 3 h, NaSeH (0.53 mmol, 55 mg) in ethanol (1 cm^3) was added and the solution was stirred for 20 h. Sodium tetraphenylborate (0.7 mmol, 240 mg) was added to the resulting brown solution, the solution was filtered, and the filtrate allowed to stand at room temperature for 5 d in the air. Brown crystals of complex **2** were obtained in 28% yield (200 mg) (Found: C, 69.2; H, 5.2. $C_{126}H_{112}B_2Ni_3P_6Se_2$ requires C, 69.8; H, 5.2%).

$[Pd_3S_2(dppe)_3][PF_6]_2$ **3**. To a stirred suspension of $Pd(MeCO_2)_2$ (0.5 mmol, 112 mg) in MeCN (15 cm^3) was added dppe (0.5 mmol, 200 mg). After 4 h NaSH (0.45 mmol, 25 mg) and triethylamine (0.3 mmol, 30 mg) were added. The solution was stirred for 20 h, treated with $NaPF_6$ (0.65 mmol, 110 mg), and filtered. The filtrate was allowed to stand for a couple of days in air. Yellow crystals of complex **3** were obtained in 17% yield (55 mg) (Found: C, 50.3; H, 3.9. $C_{78}H_{72}F_{12}P_8Pd_3S_2$ requires C, 50.1; H, 3.9%).

$[Pt_3S_2(dppe)_3][PF_6]_2$·MeCN **4**. Complex **4** was prepared by an analogous procedure to that for **3** using $PtCl_2$ (0.5 mmol, 132 mg), dppe (0.5 mmol, 200 mg), NaSH (0.8 mmol, 44 mg), NEt_3 (0.4 mmol, 40 mg), and $NaPF_6$ (0.7 mmol, 120 mg). Yellow crystals were obtained. Yield 20% (75 mg) (Found: C, 44.2; H, 3.5; N, 0.4. $C_{80}H_{75}F_{12}NP_8Pt_3S_2$ requires C, 44.2; H, 3.5; N, 0.6%).

X-Ray Crystal Structure Analysis for $[Ni_3S_2(dppe)_3][PF_6]_2$·

---

† *Supplementary data available:* see Instructions for Authors, *J. Chem. Soc., Dalton Trans.*, 1991, Issue 1, pp. xviii–xxii.

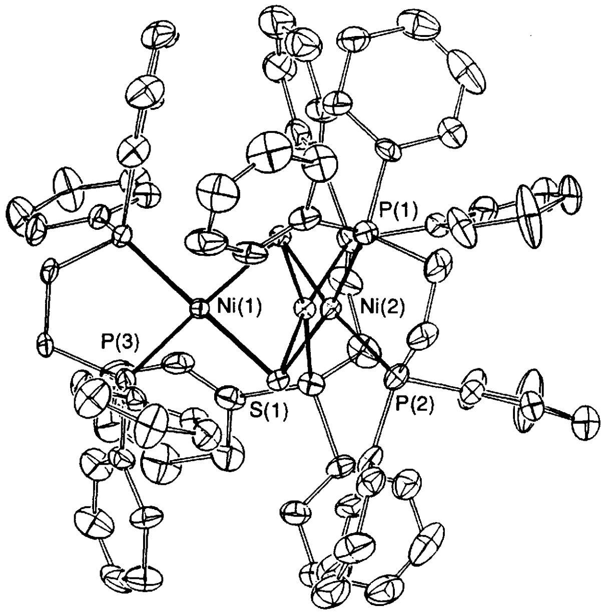

Fig. 1 A perspective view of the complex cation $[Ni_3S_2(dppe)_3]^{2+}$ of $[Ni_3S_2(dppe)_3][PF_6]_2$·MeCN with the numbering scheme

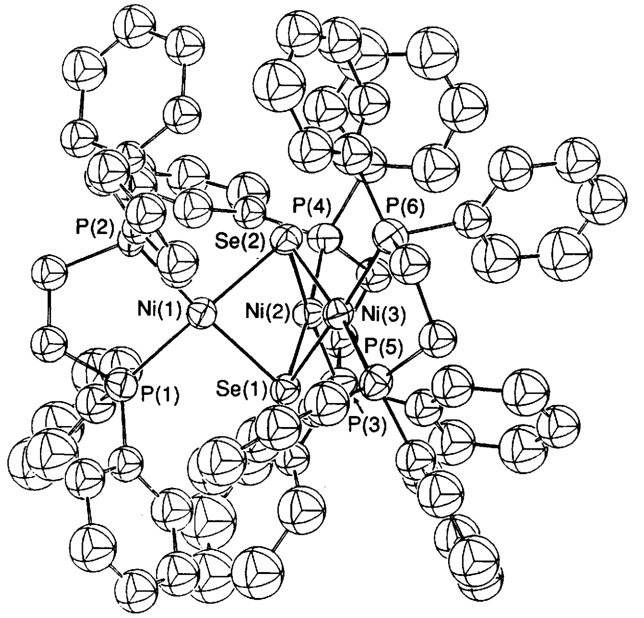

Fig. 2 A perspective view of the complex cation $[Ni_3Se_2(dppe)_3]^{2+}$ of $[Ni_3Se_2(dppe)_3][BPh_4]_2$ **2** with the numbering scheme

MeCN.—Preliminary photographic data indicated that the space group is *C*2. The space group *C*2/*m* was excluded because the unit cell contains two formula units of the complex and consequently the complex cation could not have 2/*m* symmetry in the space group *C*2/*m*. Intensity data were measured at room temperature. Three standard reflections monitored every 4 h showed no significant variation. The intensities were corrected for Lorentz polarization effects.[12] The crystal data and summary of data collection and structure refinement are given in Table 1.

Structure solution and refinement. The structure was solved by Patterson and Fourier procedures and refined by the least-squares method. Hydrogen atoms were placed at calculated positions (C–H 0.96 Å). In the final cycles of the refinement the hydrogen atoms, except for those of acetonitrile, were included with a common isotropic thermal parameter $B = 6.0$ Å^2, but their parameters were not refined. The acetonitrile molecule and the F atoms of PF_6 were isotropically refined because they are disordered. The atomic scattering factors with corrections of $\Delta f'$ for Ni, S, and P atoms were taken from ref. 13. Atomic coordinates for non-hydrogen atoms are listed in Table 2. The computer programs used for the calculations were a local version of UNICS[14] (RSLC-3, RSSFR-5, HBLS-IV, and DAPH). Figs. 1 and 2 were drawn by the use of ORTEP.[15] Calculations were performed on a HITAC M-660K computer at Osaka City University.

The X-ray structure of $[Ni_3Se_2(dppe)_3][BPh_4]$ **2** was also determined to confirm the structure. The structure was solved by the use of MULTAN 80.[16] The 11 heavy atoms were refined using the anisotropic thermal parameters and the other non-hydrogen atoms were isotropically refined because a sufficient number of high-quality intensity data was not achieved. Hydrogen atoms were, therefore, excluded from the refinement. Further details concerning the data collection and structure refinement are analogous to those for $[Ni_3S_2(dppe)_3][PF_6]_2$·MeCN. Atomic coordinates for non-hydrogen atoms are given in Table 3.

Additional material for both structures available from the Cambridge Crystallographic Data Centre comprises H-atom coordinates, thermal parameters, and remaining bond lengths and angles.

Other Measurements.—Cyclic voltammograms were recorded at 293 ± 1 and 255 ± 1 K with a Yanaco P-1100 system equipped with a Rikadenki RW201K x-y recorder. The working and counter electrodes were a glassy carbon disk and a platinum wire. The Ag–AgCl reference electrode was used in dimethylformamide (dmf) solution, the Ag–$AgClO_4$ reference electrode in acetonitrile solution. Potentials were measured against the ferrocenium–ferrocene couple as an internal standard. Tetrabutylammonium perchlorate was used as a supporting electrolyte. Acetonitrile and dimethylformamide were dried over molecular sieve type 4A and distilled.

Controlled-potential coulometry of complexes **1**–**3** was carried out at 293 ± 1 K in a standard H-type cell with a Hokuto HA-501 potentiostat and a Rikadenki RW-11T x-y recorder. The working electrode was of reticulated vitreous carbon and the counter electrode was a platinum wire. The Ag–$AgClO_4$ reference electrode was used for **1** and **2** in MeCN. Controlled-potential coulometry of **3** was carried out in dmf using the Ag–AgCl reference electrode.

Results and Discussion

The clusters **1**–**4** are air stable and soluble in organic solvents such as dichloromethane, acetonitrile, and dmf. The structure of $[Ni_3S_2(dppe)_3]^{2+}$ is shown in Fig. 1. The complex cation has a crystallographically imposed two-fold axis passing through Ni(1) and the central point between Ni(2) and Ni(2) ($-x$, y, $-z$). The overall geometry of the complex is described by three square-planar NiS_2P_2 co-ordination planes sharing two μ_3-S ligands. Each plane is tetrahedrally distorted [maximum deviation 0.22 Å for S(1)]. Selected bond lengths and angles are given in Table 4. The interesting feature of the central Ni_3S_2 core is the shorter Ni $\cdots$ Ni and longer S $\cdots$ S distances, and accordingly larger S–Ni–S angle, compared with those observed in $[Ni_3S_2(PEt_3)_6]^{2+}$,[5] indicating slimness and elongation of the central Ni_3S_2 core in the S $\cdots$ S direction. The average Ni $\cdots$ Ni length of 2.827 Å is 0.08 Å shorter and S(1) $\cdots$ S(1) ($-x$, y, $-z$) 2.924(6) Å is 0.22 Å longer than those observed in $[Ni_3S_2(PEt_3)_6]^{2+}$. The larger S–Ni–S angle of 83.7° compared with that of 77.4° in $[Ni_3S_2(PEt_3)_6]^{2+}$ may be related to the smaller P–Ni–P chelate bite angle of 88.0°. The analogous P–Ni–P angle is 98.0° in $[Ni_3S_2(PEt_3)_6]^{2+}$, where PEt_3 is monodentate. The average Ni–S bond length is 0.04 Å longer, but Ni–P is 0.1 Å shorter than those found in $[Ni_3S_2(PEt_3)_6]^{2+}$.

A view of the complex cation of **2** is shown in Fig. 2. The structure is similar to that of $[Ni_3S_2(dppe)_3]^{2+}$. The structural difference of the central Ni_3Se_2 core between **2** and

Table 1 Summary of crystal data and details of data collection and structure refinement for $[Ni_3S_2(dppe)_3][PF_6]_2 \cdot MeCN$ and $[Ni_3Se_2(dppe)_3][BPh_4]_2$ **2***

Formula	$C_{80}H_{75}F_{12}NNi_3P_8S_2$	$C_{126}H_{112}B_2Ni_3P_6Se_2$
M	1766.5	2167.8
Crystal dimensions/mm	0.45 × 0.38 × 0.30	0.50 × 0.37 × 0.18
Crystal system	Monoclinic	Triclinic
Space group	$C2$	$P\bar{1}$
a/Å	22.611(7)	29.54(3)
b/Å	14.263(3)	15.63(2)
c/Å	15.002(5)	14.39(1)
α/°		117.64(6)
β/°	125.65(3)	100.81(6)
γ/°		79.89(6)
U/Å^3	3931.2(16)	5748.0(70)
D_m/g cm^{-3}	1.47	1.24
D_c/g cm^{-3}	1.49	1.25
$F(000)$	1812	2232
μ(Mo-Kα)/cm^{-1}	9.97	4.9
$2\theta_{max}$/°	27.7	44.0
w	$1/[\sigma^2(F_o) + 0.009F_o^2]$	$1/[\sigma^2(F_o) + 0.01F_o^2]$
Maximum shift/error for last cycle	0.5	0.4
Residual electron density/e Å^{-3}	1.1	1.6
No. of reflections	$3627[2\sigma(F_o^2)]$	$5649[3\sigma(F_o^2)]$
$R[R' = (\Sigma w\Delta F^2/\Sigma wF_0^2)^{\frac{1}{2}}]$	0.070[0.102]	0.096[0.145]

* Details common to both compounds: Philips PW1100 diffractometer; Mo-Kα radiation (λ = 0.71069 Å); 22 reflections ($11 < 2\theta < 27°$) for lattice parameter determination; $Z = 2$; ω scan mode; scan rate 0.033° s^{-1}; scan range $(1.2 + 0.4 \tan\theta)°$; background time 10 s; no absorption correction; function minimized $\Sigma w(F_o - |F_c|)^2$.

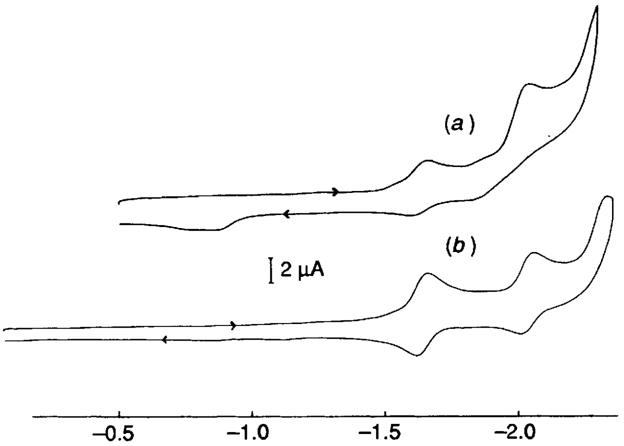

Fig. 3 Cyclic voltammograms of 3×10^{-4} mol dm^{-3} complex **1** containing 0.1 mol dm^{-3} NBu_4ClO_4 at a scan rate of 50 mV s^{-1}: (*a*) in dmf at 293 K, (*b*) in MeCN at 255 K

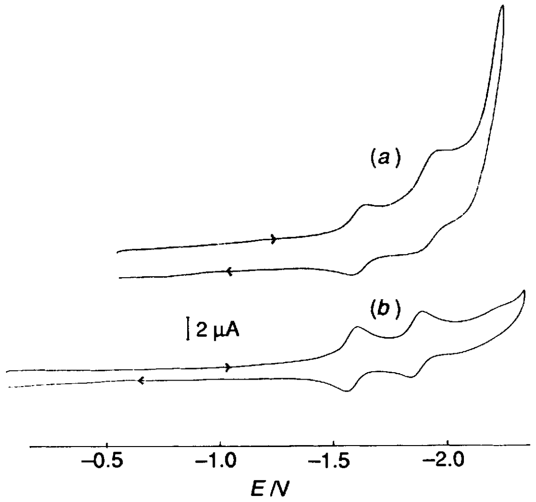

Fig. 4 Cyclic voltammograms of 3×10^{-4} mol dm^{-3} complex **2**. Conditions as in Fig. 3

$[Ni_3Se_2(PEt_3)_6]^{2+}$ [6] is analogous to that between $[Ni_3S_2(dppe)_3]^{2+}$ and $[Ni_3S_2(PEt_3)_6]^{2+}$. The Ni ··· Ni distance of 3.004 Å for **2** is 0.16 Å shorter, while the Se ··· Se distance of 3.051(4) Å is 0.18 Å longer than those for $[Ni_3Se_2(PEt_3)_6]^{2+}$. The smaller P–Ni–P angle (chelate bite) 87.2° for **2** compared with that of 101.3° for $[Ni_3Se_2(PEt_3)_6]^{2+}$ may also cause an enlargement of the Se–Ni–Se angle (82.6°) in **2**. The analogous Se–Ni–Se angle for $[Ni_3Se_2(PEt_3)_6]^{2+}$ is 76.4°. The average Ni–Se bond lengths are similar for the two complexes, while Ni–P for **2** is 0.06 Å shorter than those for $[Ni_3Se_2(PEt_3)_6]^{2+}$. Important bond lengths and angles for **2** are given in Table 5.

Structural comparison of $[Ni_3S_2(dppe)_3]^{2+}$ with $[Ni_3Se_2(dppe)_3]^{2+}$ indicates that the central Ni_3Se_2 core is slightly larger than the Ni_3S_2 core and the other bond lengths and angles are not significantly different from each other. The Ni ··· Ni separations of 2.827 Å for $[Ni_3S_2(dppe)_3]^{2+}$ and 3.004 Å for $[Ni_3Se_2(dppe)_3]^{2+}$ exclude a direct Ni ··· Ni interaction.

Numerical data from cyclic voltammograms for complexes **1**–**4** are summarized in Table 6. All potentials are reported with respect to the ferrocenium–ferrocene couple. Fig. 3 gives typical cyclic voltammograms for **1**. Two reduction peaks at −1.65 and −2.03 V are exhibited in dmf solution on an initial negative scan at 293 K. Two oxidation peaks at −1.59 and −1.83 V appear on a positive scan and moreover a broad oxidation peak at −0.87 V is observed only after cathodic scanning to −2.20 V. A couple at −1.63 V (ΔE_p = 55 mV) is reversible only after scanning to −1.80 V. Thus, the product of reduction at −2.03 V seems to be partly oxidized at −1.83 and mainly decomposed and oxidized at −0.87 V. The cyclic voltammograms of complex **1** in dmf solution at 255 K and in acetonitrile at 293 K are analogous to that in dmf at 293 K. At 255 K in MeCN two couples at −1.64 (ΔE_p = 45) and −2.04 V (ΔE_p =

Table 2 Atomic coordinates with standard deviations for $[Ni_3S_2(dppe)_3][PF_6]_2\cdot MeCN$

Atom	*x*	*y*	*z*
Ni(1)	0.0	0.000 14	0.0
Ni(2)	0.054 05(6)	0.170 31(10)	0.115 69(9)
S(1)	0.057 09(12)	0.114 90(17)	−0.017 74(18)
P(1)	0.050 01(15)	0.199 94(22)	0.254 17(21)
P(2)	0.156 05(14)	0.250 40(22)	0.201 11(22)
P(3)	0.070 14(13)	−0.107 88(19)	0.009 08(21)
C(1)	0.119 4(8)	0.288 8(11)	0.338 9(11)
C(2)	0.186 2(7)	0.265 1(12)	0.343 7(10)
C(3)	0.019 6(6)	−0.219 3(8)	−0.028 6(11)
C(11)	0.079 8(7)	0.099 8(11)	0.347 8(10)
C(12)	0.073 5(10)	0.106 9(13)	0.435 6(12)
C(13)	0.097 1(9)	0.027 6(18)	0.507 5(12)
C(14)	0.122 6(9)	−0.050 0(16)	0.490 4(14)
C(15)	0.129 6(9)	−0.054 6(15)	0.406 0(16)
C(16)	0.104 5(7)	0.022 1(11)	0.330 6(11)
C(21)	−0.035 0(7)	0.238 4(9)	0.231 5(10)
C(22)	−0.052 1(8)	0.333 6(11)	0.223 9(12)
C(23)	−0.116 3(11)	0.356 7(14)	0.207 2(17)
C(24)	−0.167 1(10)	0.291 9(15)	0.184 2(15)
C(25)	−0.149 7(8)	0.197 2(13)	0.195 9(13)
C(26)	−0.085 8(7)	0.170 7(12)	0.212 8(11)
C(31)	0.236 3(6)	0.210 9(8)	0.210 3(9)
C(32)	0.300 3(7)	0.197 0(10)	0.308 0(12)
C(33)	0.361 8(8)	0.167 9(15)	0.308 9(15)
C(34)	0.355 9(9)	0.154 6(15)	0.211 7(17)
C(35)	0.290 8(10)	0.174 7(15)	0.114 8(15)
C(36)	0.229 8(6)	0.199 6(12)	0.112 3(11)
C(41)	0.142 4(6)	0.367 0(9)	0.146 0(10)
C(42)	0.090 6(11)	0.384 9(11)	0.035 8(14)
C(43)	0.086 0(17)	0.474 5(14)	−0.007 3(17)
C(44)	0.134 8(16)	0.543 0(11)	0.064 0(26)
C(45)	0.181 3(11)	0.528 8(11)	0.173 2(17)
C(46)	0.186 3(9)	0.440 8(11)	0.211 6(16)
C(51)	0.100 2(6)	−0.101 8(9)	−0.079 0(10)
C(52)	0.054 1(7)	−0.121 7(12)	−0.188 8(10)
C(53)	0.078 2(9)	−0.111 1(16)	−0.256 2(11)
C(54)	0.145 8(9)	−0.086 8(12)	−0.215 0(13)
C(55)	0.192 9(10)	−0.067 6(14)	−0.107 7(14)
C(56)	0.172 4(7)	−0.075 1(11)	−0.037 3(11)
C(61)	0.152 6(6)	−0.118 1(8)	0.150 6(9)
C(62)	0.169 5(7)	−0.201 7(9)	0.209 3(11)
C(63)	0.230 5(8)	−0.203 0(11)	0.314 9(12)
C(64)	0.274 7(8)	−0.128 2(13)	0.363 6(11)
C(65)	0.256 8(6)	−0.042 4(11)	0.305 8(10)
C(66)	0.194 5(6)	−0.039 2(9)	0.199 1(9)
P(4)	0.091 9(2)	0.610 4(3)	0.354 6(3)
C(71)	0.0	0.459(4)	0.5
C(72)	0.0	0.358(3)	0.5
N(71)	0.0	0.281(4)	0.5
F(1)	0.069(2)	0.675(3)	0.257(3)
F(2)	0.157(2)	0.676(2)	0.431(2)
F(3)	0.046(2)	0.667(3)	0.381(3)
F(4)	0.026(2)	0.546(2)	0.281(2)
F(5)	0.137(2)	0.552(3)	0.330(3)
F(6)	0.115(2)	0.547(2)	0.453(2)

45 mV) are reversible with disappearance of the broad oxidation peak at −0.89 V. Controlled-potential coulometry for **1** in MeCN solution at −1.80 V indicates that the process involves a one-electron reduction.

The cyclic voltammogram of complex **2** in dmf at 293 K shown in Fig. 4 gives reduction peaks at −1.64 and −1.96 V and corresponding oxidation peaks at −1.58 and −1.89 V. The broad oxidation peak at −0.87 V observed for **1** is not present in this case. Two reversible couples are exhibited at 255 K in dmf solution and in MeCN solution. Controlled potential coulometry for **2** in MeCN solution at −1.70 V also indicates a one-electron reduction process. The electrode reactions for **1** and **2** in MeCN at 255 K are shown in equation (1). Though the

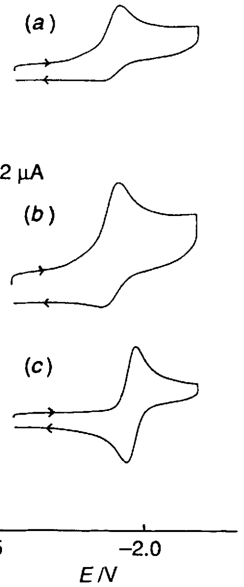

Fig. 5 Cyclic voltammograms of 3 × 10^{-4} mol dm^{-3} complex **3** in dmf containing 0.1 mol dm^{-3} NBu_4ClO_4 at (*a*) 50 mV s^{-1} at 293 K, (*b*) 100 mV s^{-1} at 293 K, and (*c*) 50 mV s^{-1} at 255 K

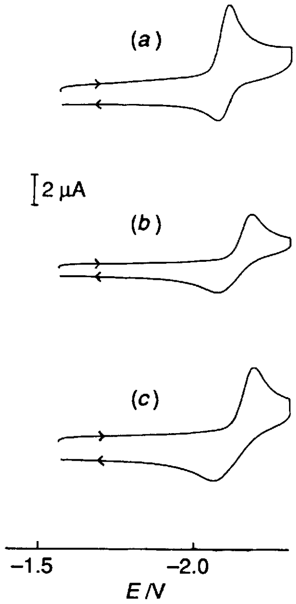

Fig. 6 Cyclic voltammograms of 3 × 10^{-4} mol dm^{-3} complex **4** in dmf containing 0.1 mol dm^{-3} NBu_4ClO_4 at (*a*) 50 mV s^{-1} at 293 K, (*b*) 50 mV s^{-1} at 255 K, and (*c*) 100 mV s^{-1} at 255 K

$$[Ni_3E_2(dppe)_3]^{2+} \rightleftharpoons [Ni_3E_2(dppe)_3]^{+} \rightleftharpoons [Ni_3E_2(dppe)_3] \qquad (1)$$

1	E = S	−1.64 V	−2.04 V
2	E = Se	−1.59 V	−1.87 V

cyclic voltammograms of **1** and **2** depend on the solvent, the complexes are reversibly reduced and oxidized in MeCN solution at 255 K. Both redox potentials of **2** are slightly higher than those of **1**, which indicates that the Se^{2-}-co-ordinated complexes $[Ni_3Se_2(dppe)_3]^{2+}$ and $[Ni_3Se_2(dppe)_3]^{+}$ are easier to reduce than the corresponding S^{2-}-containing $[Ni_3S_2(dppe)_3]^{2+}$ and $[Ni_3S_2(dppe)_3]^{+}$, though the redox potential of $[Ni(dppe)(MeC_6H_3S_2)]$ is reported to be slightly lower than that of $[Ni(dppe)(MeC_6H_3O_2)]$.[17]

In the cyclic voltammogrom of complex **3** in dmf solution (Fig. 5) a single reduction peak at −1.91 V is exhibited on the negative potential scan and on the reverse scan no oxidation peak was observed with a scan rate of 50 mV s^{-1} at 293 K, but a

Table 3 Atomic coordinates with standard deviations for $[Ni_3Se_2(dppe)_3][BPh_4]_2$ **2**

Atom	*x*	*y*	*z*	Atom	*x*	*y*	*z*
Se(1)	0.774 21(8)	0.257 13(16)	0.691 19(17)	C(60)	0.894 9(10)	0.537 9(21)	0.868 7(22)
Se(2)	0.727 32(8)	0.338 99(16)	0.891 46(17)	C(61)	0.943 9(10)	0.516 9(21)	0.891 2(22)
Ni(1)	0.790 79(10)	0.226 64(20)	0.837 75(21)	C(62)	0.966 9(10)	0.423 7(23)	0.853 4(24)
Ni(2)	0.700 93(10)	0.245 68(20)	0.717 27(21)	C(63)	0.939 9(11)	0.349 1(24)	0.793 4(24)
Ni(3)	0.763 78(10)	0.414 00(20)	0.825 33(21)	C(64)	0.889 6(10)	0.369 5(21)	0.777 2(22)
P(1)	0.844 9(3)	0.106 1(5)	0.775 3(5)	C(65)	0.741 1(9)	0.574 0(19)	1.085 4(19)
P(2)	0.810 1(2)	0.221 4(5)	0.988 5(5)	C(66)	0.783 3(10)	0.585 4(20)	1.151 0(21)
P(3)	0.674 1(3)	0.168 4(5)	0.550 5(5)	C(67)	0.781 4(12)	0.596 2(25)	1.257 0(26)
P(4)	0.634 6(2)	0.234 6(5)	0.753 1(5)	C(68)	0.736 1(10)	0.603 8(21)	1.282 9(22)
P(5)	0.806 9(3)	0.484 4(5)	0.777 8(5)	C(69)	0.696 9(10)	0.593 9(21)	1.218 2(22)
P(6)	0.745 1(3)	0.557 7(5)	0.950 1(5)	C(70)	0.698 1(9)	0.578 6(19)	1.111 3(20)
C(1)	0.817 1(9)	−0.011 0(18)	0.689 8(19)	C(71)	0.691 7(8)	0.620 0(17)	0.914 5(18)
C(2)	0.846 1(12)	−0.091 3(25)	0.631 7(26)	C(72)	0.671 5(10)	0.580 9(23)	0.815 6(24)
C(3)	0.821 5(12)	−0.177 9(26)	0.572 0(26)	C(73)	0.631 6(12)	0.631 2(26)	0.775 7(27)
C(4)	0.778 0(11)	−0.177 2(25)	0.574 6(26)	C(74)	0.614 9(11)	0.725 0(23)	0.857 1(24)
C(5)	0.749 5(11)	−0.100 2(24)	0.635 4(25)	C(75)	0.636 7(10)	0.766 3(21)	0.958 5(22)
C(6)	0.773 2(9)	−0.008 5(20)	0.690 2(21)	C(76)	0.675 2(9)	0.712 2(21)	0.989 9(21)
C(7)	0.888 2(8)	0.105 0(16)	0.699 2(17)	C(77)	0.793 7(8)	0.616 4(17)	0.850 9(18)
C(8)	0.870 3(9)	0.103 5(20)	0.597 6(20)	C(78)	0.786 8(9)	0.638 0(19)	0.970 5(19)
C(9)	0.904 6(9)	0.107 8(20)	0.538 5(21)	C(79)	0.469 4(8)	0.392 2(17)	0.618 6(18)
C(10)	0.950 5(9)	0.100 1(20)	0.571 3(21)	C(80)	0.502 9(8)	0.410 0(17)	0.576 5(18)
C(11)	0.965 1(10)	0.098 5(22)	0.663 1(23)	C(81)	0.519 6(9)	0.503 0(19)	0.627 0(20)
C(12)	0.934 4(8)	0.102 4(18)	0.736 4(19)	C(82)	0.505 9(9)	0.575 6(19)	0.721 7(20)
C(13)	0.848 4(7)	0.316 0(15)	1.072 1(16)	C(83)	0.472 5(9)	0.554 8(19)	0.767 4(20)
C(14)	0.863 6(7)	0.366 2(16)	1.027 3(17)	C(84)	0.455 6(9)	0.461 5(18)	0.716 8(19)
C(15)	0.895 2(9)	0.436 6(19)	1.095 3(20)	C(85)	0.471 6(7)	0.207 6(15)	0.469 4(16)
C(16)	0.907 4(9)	0.457 5(18)	1.196 5(19)	C(86)	0.491 1(8)	0.117 3(16)	0.467 3(17)
C(17)	0.892 4(9)	0.409 7(20)	1.240 7(20)	C(87)	0.513 2(8)	0.041 9(17)	0.382 1(17)
C(18)	0.861 8(8)	0.337 8(17)	1.180 1(18)	C(88)	0.519 3(8)	0.059 8(18)	0.296 6(19)
C(19)	0.769 1(7)	0.233 0(15)	1.072 2(16)	C(89)	0.499 7(9)	0.146 6(19)	0.293 0(20)
C(20)	0.744 1(8)	0.325 4(17)	1.120 9(18)	C(90)	0.474 5(9)	0.221 7(20)	0.381 0(20)
C(21)	0.709 2(8)	0.342 0(18)	1.191 2(19)	C(91)	0.389 7(8)	0.310 4(17)	0.507 6(18)
C(22)	0.701 2(9)	0.259 5(19)	1.201 8(21)	C(92)	0.369 6(10)	0.244 8(22)	0.414 6(23)
C(23)	0.726 8(9)	0.171 5(20)	1.153 8(21)	C(93)	0.325 3(12)	0.259 9(26)	0.371 6(27)
C(24)	0.761 5(8)	0.151 4(17)	1.082 7(18)	C(94)	0.298 5(10)	0.346 7(23)	0.420 6(24)
C(25)	0.880 5(8)	0.092 0(17)	0.890 4(17)	C(95)	0.317 2(10)	0.413 3(23)	0.519 0(23)
C(26)	0.845 7(8)	0.107 0(17)	0.965 5(17)	C(96)	0.364 3(10)	0.398 5(21)	0.564 9(22)
C(27)	0.651 3(8)	0.250 9(17)	0.492 3(18)	C(97)	0.441 4(8)	0.255 4(16)	0.656 3(17)
C(28)	0.660 7(9)	0.342 6(19)	0.553 7(20)	C(98)	0.477 0(8)	0.266 2(18)	0.731 9(18)
C(29)	0.636 6(10)	0.417 9(22)	0.520 3(23)	C(99)	0.475 9(10)	0.240 7(20)	0.816 2(21)
C(30)	0.608 5(9)	0.385 0(20)	0.420 0(20)	C(100)	0.439 4(9)	0.205 3(19)	0.817 7(20)
C(31)	0.602 9(10)	0.287 6(23)	0.360 8(24)	C(101)	0.403 3(10)	0.190 0(22)	0.742 8(23)
C(32)	0.625 5(10)	0.213 2(21)	0.392 8(22)	C(102)	0.403 9(8)	0.215 7(18)	0.653 4(19)
C(33)	0.708 7(8)	0.070 1(16)	0.459 6(17)	C(103)	0.848 9(8)	−0.112 3(18)	0.038 1(19)
C(34)	0.744 1(10)	0.095 3(22)	0.424 2(23)	C(104)	0.848 8(9)	−0.138 6(19)	−0.071 2(20)
C(35)	0.777 0(11)	0.011 2(25)	0.353 5(26)	C(105)	0.804 4(10)	−0.154 5(22)	−0.138 4(23)
C(36)	0.771 6(12)	−0.085 2(25)	0.327 7(26)	C(106)	0.767 1(10)	−0.141 8(22)	−0.102 8(23)
C(37)	0.733 6(13)	−0.100 0(28)	0.366 0(29)	C(107)	0.764 2(9)	−0.112 7(20)	0.006 2(21)
C(38)	0.702 1(10)	−0.021 2(21)	0.431 7(22)	C(108)	0.806 5(8)	−0.101 4(18)	0.073 2(19)
C(39)	0.608 1(8)	0.344 4(17)	0.856 0(18)	C(109)	0.943 0(8)	−0.132 6(17)	0.053 8(17)
C(40)	0.614 9(10)	0.343 1(21)	0.957 4(21)	C(110)	0.953 6(10)	−0.087 8(21)	0.000 0(22)
C(41)	0.597 8(12)	0.433 4(25)	1.036 6(26)	C(111)	0.991 9(10)	−0.127 4(21)	−0.069 7(22)
C(42)	0.573 9(11)	0.514 2(25)	1.018 4(26)	C(112)	1.017 5(10)	−0.207 2(22)	−0.067 0(23)
C(43)	0.573 5(10)	0.507 6(23)	0.925 5(24)	C(113)	1.010 2(9)	−0.251 8(20)	−0.010 4(21)
C(44)	0.590 3(10)	0.424 2(22)	0.836 7(23)	C(114)	0.973 6(9)	−0.216 6(20)	0.046 6(21)
C(45)	0.635 8(7)	0.134 9(16)	0.784 9(16)	C(115)	0.898 3(8)	−0.145 2(16)	0.197 8(17)
C(46)	0.675 1(8)	0.113 6(18)	0.842 5(19)	C(116)	0.888 5(9)	−0.245 9(20)	0.145 8(21)
C(47)	0.676 2(9)	0.037 9(20)	0.869 9(21)	C(117)	0.890 3(10)	−0.296 5(22)	0.210 7(23)
C(48)	0.639 7(9)	−0.015 2(20)	0.838 9(21)	C(118)	0.900 2(9)	−0.250 6(20)	0.315 7(21)
C(49)	0.601 1(9)	0.002 3(20)	0.780 4(20)	C(119)	0.914 4(11)	−0.154 2(23)	0.367 1(24)
C(50)	0.596 9(9)	0.080 4(20)	0.756 3(21)	C(120)	0.909 3(9)	−0.100 8(19)	0.304 0(20)
C(51)	0.619 1(8)	0.119 7(17)	0.546 3(18)	C(121)	0.899 5(7)	0.025 4(16)	0.200 5(16)
C(52)	0.592 9(8)	0.202 8(16)	0.630 5(17)	C(122)	0.858 7(9)	0.089 5(19)	0.238 5(20)
C(53)	0.803 5(9)	0.461 4(18)	0.638 6(19)	C(123)	0.861 0(9)	0.189 3(20)	0.318 8(21)
C(54)	0.830 6(10)	0.517 1(21)	0.625 5(22)	C(124)	0.905 2(10)	0.216 6(22)	0.352 9(23)
C(55)	0.827 0(11)	0.495 6(24)	0.506 2(24)	C(125)	0.946 5(10)	0.161 6(23)	0.321 6(24)
C(56)	0.798 2(10)	0.434 4(21)	0.431 1(22)	C(126)	0.942 6(9)	0.061 8(21)	0.240 2(21)
C(57)	0.768 9(10)	0.383 7(21)	0.451 1(22)	B(1)	0.445 2(10)	0.293 4(22)	0.565 3(23)
C(58)	0.772 5(9)	0.399 1(18)	0.563 0(19)	B(2)	0.897 2(9)	−0.089 8(19)	0.121 7(20)
C(59)	0.867 5(8)	0.461 3(16)	0.810 6(17)				

small oxidation peak corresponding to the reduction peak appears at a scan rate of 100 mV s^{-1}. Controlled-potential coulometry at -2.10 V indicates that the process contains a two-electron reduction at 293 K. A couple at -1.96 V (ΔE_p = 30 mV) is reversible at 255 K. These observations suggest the presence of a chemical reaction following the reduction process.

Table 4 Selected interatomic distances (Å) and angles (°) for [Ni_3S_2(dppe)$_3$][PF_6]$_2$·MeCN

Ni(1)–S(1)	2.195(4)	Ni(1) ··· Ni(2)	2.815(3)
Ni(1)–P(3)	2.158(4)	Ni(2)–S(1$^{\mathrm{I}}$)	2.190(3)
Ni(2)–S(1)	2.190(3)	Ni(2) ··· Ni(2$^{\mathrm{I}}$)	2.852(3)
Ni(2)–P(1)	2.173(4)	S(1) ··· S(1$^{\mathrm{I}}$)	2.924(6)
Ni(2)–P(2)	2.196(4)		
P(1)–Ni(2)–P(2)	87.48(13)	S(1)–N(2) ··· S(1$^{\mathrm{I}}$)	83.77(11)
Ni(1)–S(1)–Ni(2)	79.88(11)	P(3)–Ni(1)–P(3$^{\mathrm{I}}$)	88.87(13)
Ni(1)–Ni(2)–Ni(2$^{\mathrm{I}}$)	59.57(5)	Ni(2)–S(1)–Ni(2$^{\mathrm{I}}$)	81.26(10)
Ni(2)–Ni(1)–Ni(2$^{\mathrm{I}}$)	60.87(5)	P(1)–Ni(2)–S(1$^{\mathrm{I}}$)	92.32(12)
S(1)–Ni(1)–S(1$^{\mathrm{I}}$)	83.54(11)	Ni(1)–S(1$^{\mathrm{I}}$)–Ni(2)	79.89(10)

Symmetry code: I, $-x, y, -z$.

Table 5 Selected interatomic distances (Å) and angles (°) for [Ni_3Se_2(dppe)$_3$][BPh_4]$_2$ **2**

Se(1) ··· Se(2)	3.051(4)	Ni(1) ··· Ni(3)	2.976(5)
Se(1)–Ni(1)	2.318(4)	Ni(1)–P(1)	2.195(8)
Se(1)–Ni(2)	2.315(4)	Ni(1)–P(2)	2.172(8)
Se(1)–Ni(3)	2.323(4)	Ni(2) ··· Ni(3)	3.102(5)
Se(2)–Ni(1)	2.307(4)	Ni(2)–P(3)	2.186(9)
Se(2)–Ni(2)	2.300(4)	Ni(2)–P(4)	2.172(8)
Se(2)–Ni(3)	2.302(4)	Ni(3)–P(5)	2.194(8)
Ni(1) ··· Ni(2)	2.935(5)	Ni(3)–P(6)	2.183(8)
Ni(1)–Se(1)–Ni(2)	78.60(14)	Se(1)–i(2)–Se(2)	82.77(14)
Ni(1)–Se(1)–Ni(3)	79.74(14)	Se(1)–Ni(2)–P(3)	96.9(3)
Ni(2)–Se(1)–Ni(3)	83.93(14)	Se(2)–Ni(2)–P(4)	93.6(3)
Ni(1)–Se(2)–Ni(2)	79.14(14)	Ni(1)–Ni(2)–Ni(3)	58.99(10)
Ni(1)–Se(2)–Ni(3)	80.41(13)	P(3)–Ni(2)–P(4)	86.9(3)
Ni(2)–Se(2)–Ni(3)	84.74(14)	Se(1)–Ni(3)–Se(2)	82.54(13)
Se(1)–Ni(1)–Se(2)	82.54(13)	Se(1)–Ni(3)–P(5)	98.6(3)
Se(1)–Ni(1)–P(1)	96.6(3)	Se(2)–Ni(3)–P(6)	92.2(3)
Se(2)–Ni(1)–P(2)	94.5(3)	Ni(1)–Ni(3)–Ni(2)	57.71(10)
Ni(2)–Ni(1)–Ni(3)	63.30(11)	P(5)–Ni(3)–P(6)	87.3(3)
P(1)–Ni(1)–P(2)	87.5(3)		

Table 6 Numerical data from cyclic voltammograms of complexes **1**–**4** (3 × 10^{-4} mol dm^{-3}) containing 0.1 mol dm^{-3} NBu_4ClO_4 at a scan rate of 50 mV s^{-1}

Complex	Solvent	E_{pa}/V	E_{pc}/V	E_{pa}/V	ΔE_p/mV	E_{pc}/V	E_{pa}/V	ΔE_p/mV
1 [Ni_3S_2(dppe)$_3$][BPh_4]$_2$·MeCN*	dmf	-0.87	-1.65	-1.59		-2.03	-1.83	
		(-0.67)	(-1.68)	(-1.63)		(-2.04)	(-1.85)	
	MeCN	-0.89	-1.65	-1.60	55	-2.08	-2.02	
			(-1.66)	(-1.62)	(45)	(-2.06)	(-2.01)	(45)
2 [Ni_3Se_2(dppe)$_3$][BPh_4]$_2$*	dmf		-1.64	-1.58		-1.96	-1.89	
			(-1.66)	(-1.61)	(50)	(-1.93)	(-1.87)	(65)
	MeCN		-1.62	-1.56	60	-1.95	-1.88	
			(-1.61)	(-1.56)	(50)	(-1.89)	(-1.84)	(50)

		293 K		255 K		
		E_{pc}/V	E_{pa}/V	E_{pc}/V	E_{pa}/V	ΔE_p/mV
3 [Pd_3S_2(dppe)$_3$][PF_6]$_2$	dmf	-1.91		-1.97	-1.94	30
4 [Pt_3S_2(dppe)$_3$][PF_6]$_2$·MeCN	dmf	-2.10	-2.07	-2.18	-2.07	

* Values at 293 K; those in parentheses refer to 255 K.

A reduction peak at -2.10 V with associated smaller oxidation peak at -2.07 V is present in the voltammogram of complex **4** at a scan rate of 50 mV s^{-1} (ΔE_p = 30 mV) in dmf solution at 293 K (Fig. 6). An analogous cyclic voltammogram was observed at scan rates from 50 to 500 mV s^{-1} (ΔE_p = 60 mV), though the peak-to-peak separation is larger at higher scan rates. The process is considered as a two-electron transfer because the cyclic voltammograms of **3** and **4** show an almost identical cathodic peak current i_{pc}. At 255 K an analogous couple to that at 293 K is observed at a scan rate of 50 mV s^{-1} (ΔE_p = 100 mV). The peak-to-peak separation is much larger at higher scan rate and ΔE_p = 150 mV was obtained at 200 mV s^{-1}. Therefore, the reaction of complex **4** on the electrode surface is slow.

As in the case of mononuclear complexes,[18] **1** and **2** are easier to reduce than **4** or **5**. The ease of reduction follows the order Ni > Pd > Pt in these complexes. The S^{2-}-co-ordinated complex **1** is more difficult to reduce than the Se^{2-}-containing **2**.

Acknowledgements

The authors thank Dr. A. Ichimura for valuable suggestions and Mr. Jyun-ichi Gohda for elemental analyses.

References

1 W. Tremel, B. Krebs and G. Henkel, *Inorg. Chim. Acta*, 1983, **80**, L31.
2 G. Henkel, M. Kriege and K. Matsumoto, *J. Chem. Soc., Dalton Trans.*, 1988, 657.
3 K. Matsumoto, M. Nakano and S. Ooi, *Chem. Lett.*, 1988, 823.
4 W. Tremel and G. Henkel, *Inorg. Chem.*, 1988, **27**, 3896.
5 C. A. Ghilardi, S. Midollini and L. Sacconi, *Inorg. Chim. Acta*, 1978, **31**, L431.
6 F. Cecconi, C. A. Ghilardi and S. Midollini, *Inorg. Chem.*, 1983, **22**, 3802.
7 C. A. Ghilardi, S. Midollini, A. Orlandini, C. Battistoni and G. Mattogno, *J. Chem. Soc., Dalton Trans.*, 1984, 939.
8 C. A. Ghilardi, P. Innocenti, S. Midollini and A. Orlandini, *J. Chem. Soc., Dalton Trans.*, 1985, 2209.
9 F. Cecconi, C. A. Ghilardi, S. Midollini, A. Orlandini, A. Vacca and J. A. Ramirez, *J. Chem. Soc., Dalton Trans.*, 1990, 773.
10 F. Fehér in *Handbuch der präparativen Anorganischen Chemie*, ed. G. Brauer, Ferdinand Enke Verlag, Stuttgart, 1954, vol. 1, p. 278.
11 D. L. Klayman and T. S. Griffin, *J. Am. Chem. Soc.*, 1973, **95**, 197.
12 J. Hornstra and B. Stubbe, PW1100 Data Processing Programs, Philips Research Laboratories, Eindhoven, 1972.
13 *International Tables for X-Ray Crystallography*, Kynoch Press, Birmingham, 1974, vol. 4, pp. 99 and 149.
14 The Universal Crystallographic Computation Program System, The Crystallographic Society of Japan, Tokyo, 1968.

15 C. K. Johnson, ORTEP II, Report ORNL-5138, Oak Ridge National Laboratory, Oak Ridge, TN, 1976.

16 P. Main, S. J. Fiske, S. E. Hull, L. Lessinger, G. Germain, J.-P. Declercq and M. M. Woolfson, MULTAN 80, A System of Computer Programs for the Automatic Solution of Crystal Structures from X-Ray Diffraction Data, Universities of York, England, and Louvain, Belgium.

17 G. A. Bowmaker, P. D. W. Boyd and G. K. Campbell, *Inorg., Chem.*, 1982, **21**, 2403.

18 R. L. Cowan, D. B. Pourreau, A. L. Rheingold, S. J. Geib and W. C. Trogler, *Inorg. Chem.*, 1987, **26**, 259.

Received 10*th September* 1990; *Paper* 0/04104A